

## SSC DIPOLE MAGNET CRYOSTAT THERMAL MODEL MEASUREMENT RESULTS

R.C. Niemann, W.N. Boroski, J.D. Gonczy, T.H. Nicol,  
J.G. Otavka and M.K. Ruschman

Fermi National Accelerator Laboratory  
Batavia, Illinois

R.J. Powers

Powers Associates, Inc.  
Swampscott, Massachusetts

### ABSTRACT

Thermal performance of the conceptual design SSC dipole magnet cryostat has been experimentally evaluated. A full scale thermal model was constructed and open cycle thermal performance measurements were made. Details of the measurement program, measurement results and a comparison of predicted and measured performance are presented. The measurement methods and improvements of them for possible follow-on evaluations are discussed.

### INTRODUCTION

The SSC dipole magnet development program includes the design, construction and testing of superconducting magnet models.<sup>1</sup> The model program is structured to provide information and to gain experience with design features, fabrication, handling and operational performance, both magnetic and cryogenic.

As a precursor to the construction of actual magnet models, a full length (17.5m) thermal model was built. The objectives of the thermal model program were to utilize and improve the magnet production facility and manufacturing procedures, to evaluate the cryostat design from a production standpoint, to gain experience in magnet handling and transportation, to monitor the transient thermal and structural responses of the cryostat and to measure the heat leaks to the cold mass and the thermal shields.

### CRYOSTAT

The cryostat design has been previously described in detail<sup>2</sup> and thus only its major features are presented herein. The cryostat general arrangement is as shown by Fig. 1 and 2.

#### Cold Mass Assembly

The cold mass assembly consists of the beam tube, magnetic correction elements, collared coils, laminated iron yoke and outer helium containment shell.

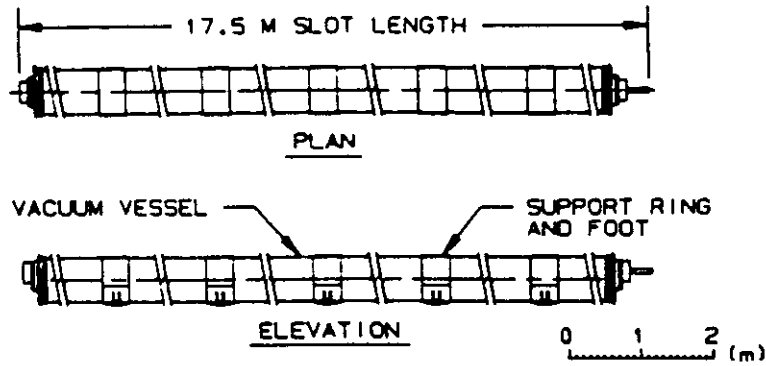


Fig. 1. Cryostat plan and elevation views.

The cold mass components are joined together forming a leak-tight and structurally rigid assembly.

### Cryogenic Piping

The cryostat assembly contains all piping that interconnects the magnet refrigeration system throughout the circumference of the accelerator rings. A five pipe system is employed for cryogenic and safety reasons.

### Thermal Shields

Thermal shields maintained independently at 20 and 80 K surround the cold mass assembly. The shields absorb the radiant heat flux and provide heat sink stations for the suspension system. The shields are supported by and thermally connected to the cold mass assembly supports.

### Insulation

Insulation is installed on the external surfaces of the inner and outer shields. The insulation consists of blankets of flat, reflective radiation shields with mat spacers.<sup>3</sup> One blanket is installed on the inner shield and four are installed on the outer shield.

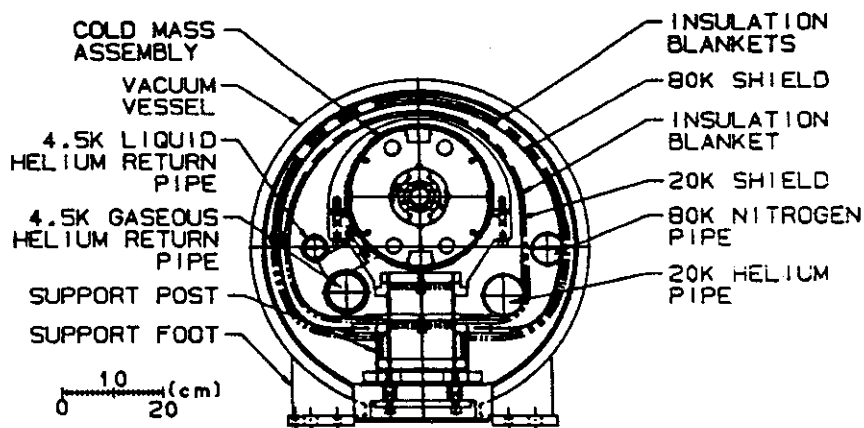


Fig. 2. Cryostat cross section at a suspension point.



The measurements were performed in an open cycle mode. The cold mass was supplied liquid helium by reservoirs at each end. The inner shield was supplied helium from an external dewar. Since the inner shield temperature was an operational variable, its value was controlled by varying the flowrate through the shield. The outer shield was supplied liquid nitrogen by reservoirs at each end. The external piping was equipped to measure the flowrates of the cold mass, inner shield and outer shield gas streams.

After cooldown, initial filling and general stabilization of the three systems, the temperature of the inner shield was regulated to a selected test value. After regulation, temperatures and heat leaks at each system were monitored to establish equilibrium. The equilibration process for each operating point required several days. Once at equilibrium, steady state heat leak data was taken.

### Cold Mass

The cold mass heat leak was determined from boiloff measurements. Since the measurement includes the heat leaks of both the cold mass and the end reservoirs, a separate measurement of the end reservoir heat leak was made and then subtracted from the total measured heat leak.

### Inner Shield

The inner shield heat leak was determined from the shield gas stream heating. The flowrate through the shield and the helium  $\Delta T$  along the shield were monitored.

### Outer Shield

The outer shield heat leak was determined from boiloff measurements. Like the cold mass measurements, an end reservoir heat leak subtraction was employed.

## RESULTS

The experimental program extended for ~3 months and involved 23 data taking runs as identified by the inner shield temperature. The following results have been screened to exclude transient periods, upset conditions and operational problems.

### Cooldown

Cooldown was gradual due to the open cycle nature of the operation. The cold mass was initially cooled and filled with liquid nitrogen, evacuated and then filled with liquid helium. The total time required to cool and fill the cold mass with liquid helium was 294 hrs.

The support post bending loads due to differential axial thermal contraction were low with the exception of the downstream end post which indicated a load of 4800N. A probable cause for such a load is a nonoperational; i.e., binding, cold mass slide. The support post temperature profiles agreed well with those of an identical post measured in a heat leak test facility.<sup>7</sup>

Random mechanical noises occurred during cooldown and throughout the measurement program. A probable cause of such noises is relative motions between the cold mass and/or shields and support posts as a result of vacuum vessel motions due to ambient temperature variations and/or settling of the test pad.

### Cold Mass

The subtractive heat leak contribution of the end reservoirs was measured with the inner shield cooling tube filled with liquid helium to eliminate conduction and thermal radiation to the cold mass end to include end shine thermal radiation. Under these conditions, the shield temperature was 7.6 K and the measured background was 865 mW. The background was not strongly dependent on reservoir liquid level.

Calibration heaters in the cold mass were employed to evaluate the accuracy of the measurement system. The heaters were energized with the inner shield at ~20 K. The measured heat leak increases corresponding to heater power levels of 200 mW and 398 mW were 197 mW and 376 mW, respectively.

The cold mass heat leak at the cryostat design point; i.e., inner shield operating at 20 K, was  $140 \pm 40$  mW as compared to the predicted 128 mW and the budgeted 300 mW. The cold mass heat leak vs inner shield temperature is given by Fig. 4.

Considerable differences exist between measured and predicted heat leaks at several experimental points. Factors that can contribute to these differences are as follow:

- The center section heat leak (140 mW) is small relative to the balance of the apparatus (865 mW). This unbalance amplifies end vessel effects.
- Thermal communication exists between the inner shield cooling circuit and the end vessel helium reservoirs as a result of the inner shield supply and return piping passing through the cold mass helium reservoirs. Even though the piping was insulated, transients in inner shield supply conditions could be seen to affect the reservoirs.
- Level instability (sloshing) occurred occasionally in the end vessels. The sloshing was most often associated with changes in the inner shield circuit operation.
- The predicted sensitivity to insulating vacuum is high. At the design inner shield operating temperature of 20 K, the residual gas (helium) conduction at  $10^{-6}$  torr is 43 mW and at  $10^{-5}$  torr is 430 mW. The insulating vacuum at the vacuum vessel midspan port ranged from  $1.3 \times 10^{-6}$  to  $2.9 \times 10^{-6}$  torr during the span of the measurements. The location and installation of the vacuum gauge was demonstrated by diagnostic measurements to inaccurately relate changes in the insulating vacuum that could correspond to changes in the outgassing rate of the mild steel vacuum vessel due to changes in ambient temperature. Consequently, vacuum was not monitored frequently during most of the data taking.
- Variations in atmospheric pressure result in temperature changes of the liquid which influence the apparent heat leak. Atmospheric pressure was not monitored frequently during most of the data taking. Where possible, the heat leak was corrected for changes of liquid temperature and pressure with time. The cold mass end to end temperature variation during operation was characteristically  $\pm 30$  mK.

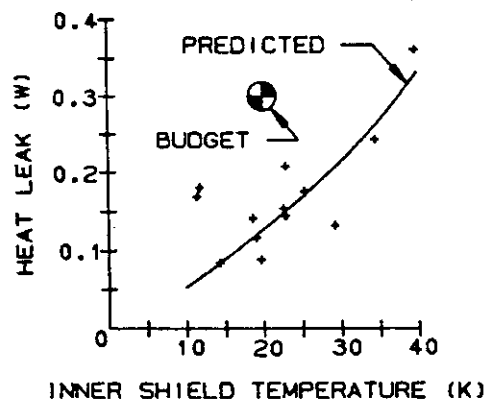


Fig. 4. Measured cold mass heat leak.

The inner shield heat leak at the cryostat design point was  $5.0 \pm 0.4$  W as compared to the predicted 2.77 W and the budgeted 2.5 W. The inner shield heat leak vs inner shield temperature is given by Fig. 5.

A corroboration of the inner shield heat leak measurement was provided by performing inner shield boiloff measurements during the cold mass background measurement. With the shield cooling tube filled with liquid helium, the heat leak as measured by boiloff was 5.64 W.

The factor of two difference between measured and predicted heat leaks is felt to be due to thermal shorts between the 20 and 80 K systems, by locally compressed insulation between the shields and by an insufficient number of layers of insulation. Shield and support temperature monitors indicate the possibility of shorts. An autopsy of the thermal model to investigate the existence of such thermal shorts has not been conducted for programmatic reasons.

### Outer Shield

The subtractive heat leak contribution of the end reservoirs was made with the center section removed and the reservoirs connected together. The nominal background heat leak was  $\sim 24$  W. The background was found to vary with level; i.e.,  $\sim 3$  W for a level change from "full" to "half" and accordingly a variable subtraction was employed. The outer shield heat leak at the cryostat design point was  $19 \pm 2$  W compared to the predicted 23.3 W and the budgeted 25 W. The outer shield heat leak vs inner shield temperature data is given by Fig. 6. The less than predicted measured heat leaks are felt to be associated with the thermal shorts that are suspected exist between the inner and outer shields and their connections. The scatter in the measured heat leak is felt to be associated with the sensitivity of the insulation systems to insulating vacuum<sup>8</sup> in the higher pressure ranges; i.e.,  $>10^{-4}$  Torr. As noted earlier, the insulating vacuum, while not accurately measured, showed changes with ambient temperature.

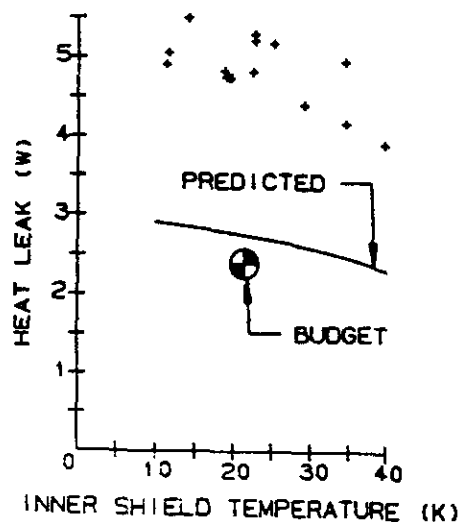


Fig. 5. Measured inner shield heat leak.

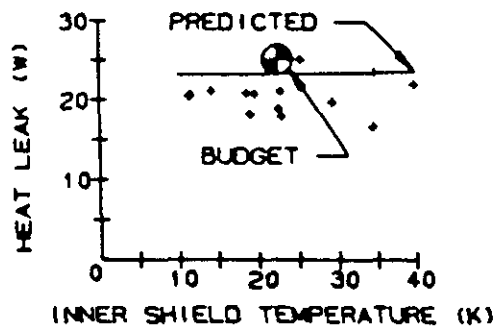


Fig. 6. Measured outer shield heat leak.

## IMPROVEMENTS FOR FOLLOWON MEASUREMENTS

### Methods

The measurements of the cold mass and outer shield heat leaks were indirect since they included the measurement of an associated background which in both cases was large. Direct measurements that involve devices such as heatmeters<sup>9</sup> would improve the measurements and should be evaluated for their accuracy and suitability to the model measured.

### Thermal Model

For the same experimental method, the model requires several changes. The backgrounds should be reduced significantly by incorporating low heat end vessels. The inner shield cooling circuit should be totally separate from the cold mass circuit. Placement of pressure and vacuum measurement transducers should be improved.

### Instrumentation

All transducer signals should be directly inputted to the computer driven data acquisition system to permit total on-line data processing and evaluation of transients, upset conditions, etc. Pressure and vacuum monitoring should be expanded to include end vessels, interior regions of the model, etc.

### Protocol

Background measurements should be expanded to establish the effects of operating pressure, insulating vacuum and liquid level. Transient performance criteria should be evaluated and updated.

### Component Measurements

Measurements of cryostat components that contribute to the heat leak; i.e., insulation, support posts, etc. should continue to be made. Operation at off-design conditions should be included.

### Analytical Model

The analytical model for the cryostat should continue to be improved in the areas of transient and off-design conditions. Model inputs should include factors generated by component evaluations. Correlations of the physical and analytical model should be ongoing.

## CONCLUSIONS

- The measurement methods are appropriate.
- The model, instrumentation and protocol can be improved in a straightforward manner to improve measurement results.

- The cryostat, with the possible exception of a cold mass slide, performed well during cooldown and steady state operation.
- With the exception of the inner shield, the measured heat leaks were within budget. The temperature monitors on the model indicated possible shorts between the inner and outer shields.
- The thermal measurements indicate that the superconducting magnets for the SSC can be built within the heat leak budgets as required for accelerator operation.

## ACKNOWLEDGEMENTS

The authors gratefully acknowledge the sincere interest, extensive contributions and diligent performance of the many Fermilab design, magnet production and engineering test personnel. Their combined efforts resulted in the design, construction and test of a dipole magnet cryostat that answers the cryogenic needs of the SSC. The work as presented was performed at Fermi National Accelerator Laboratory which is operated by Universities Research Association Inc., under contract with the U.S. Department of Energy.

## REFERENCES

1. SSC Central Design Group, Conceptual design of the superconducting super collider, "SSC-SR-2020," March 1986.
2. R.C. Niemann, et al, Superconducting super collider magnet cryostat, cryogenic properties, "Processes and Applications," No. 251, Vol. 82, p. 136, (1986).
3. T. Ohmori, et al, Thermal performance of candidate SSC magnet cryostat thermal insulation systems, "Adv. Cryo. Engr.," 33, Plenum Press, New York (to be published).
4. T.H. Nicol, et al, SSC magnet cryostat suspension system design and performance, "Adv. Cryo. Engr.," 33, Plenum Press, New York (to be published).
5. R.C. Niemann, et al, Design, construction and test of a full scale SSC dipole magnet cryostat thermal model, "Applied Superconductivity Conference," September 30 - October 3, 1986 in Baltimore, Maryland (to be published).
6. N.H. Engler, et al, SSC long dipole magnet model construction experience, "Adv. Cryo. Engr.," 33, Plenum Press, New York (to be published).
7. J.D. Gonczy, et al, Cryogenic support thermal performance measurements, "Adv. Cryo. Engr.," 33, Plenum Press, New York (to be published).
8. T. Ohmori, et al, Thermal performance of candidate SSC magnet cryostat thermal insulation systems, "Adv. Cryo. Engr.," 33 Plenum Press, New York (to be published).
9. M. Kuchnir, et al, Measuring heat leak with a heatmeter, "Adv. Cryo. Engr.," 31, (1986) Plenum Press, New York.